PLOS Complex Systems

RESEARCH ARTICLE

Characterization of monotone Boolean models supporting fixed points and multistability in balanced networks

Sarah Adigwe[1☯], **Harshavardhan BV**[2☯], **Mohit Kumar Jolly**[3], **Tomáš Gedeon**[1*]

1 Department of Mathematical Sciences, Montana State University, Bozeman, Montana, United States of America, **2** IISc Mathematics Initiative, Indian Institute of Science, Bengaluru, India, **3** Department of Bioengineering, Indian Institute of Science, Bengaluru, India

☯ These authors contributed equally to this work.
* tgedeon@montana.edu

OPEN ACCESS

Citation: Adigwe S, BV H, Jolly MK, Gedeon T (2026) Characterization of monotone Boolean models supporting fixed points and multistability in balanced networks. PLOS Complex Syst 3(5): e0000103. https://doi.org/10.1371/journal.pcsy.0000103

Editor: Vera Pancaldi, INSERM U1037, FRANCE

Received: October 17, 2025

Accepted: March 21, 2026

Published: May 7, 2026

Peer Review History: PLOS recognizes the benefits of transparency in the peer review process; therefore, we enable the publication of all of the content of peer review and author responses alongside final, published articles. The editorial history of this article is available here: https://doi.org/10.1371/journal.pcsy.0000103

Abstract

Gene regulatory networks (GRN) control the expression levels of proteins in cells, and understanding their dynamics is key to potentially controlling disease processes. Steady states of GRNs are interpreted as cellular phenotypes, and the first step in understanding GRN dynamics is describing the collection of steady states the network can support in different conditions. We consider a collection of all monotone Boolean function models compatible with a given GRN, and ask which steady states are supported by most models. We find that for balanced networks, there is an explicit hierarchy in the prevalence of individual steady states, as well as the prevalence of bistability and multistability. The key insight that we use is that monotone Boolean models supporting a given equilibrium are a product of prime ideals and prime filters of the lattices of monotone Boolean functions. To illustrate our result, we show that in the EMT network associated with cancer metastasis, the most common equilibria correspond to epithelial (E) and mesenchymal (M) states, and the bistability between them is the most common bistability among all network-compatible monotone Boolean models.

Author summary

Cells adjust their behavior in response to external inputs via networks of genes that regulate each other's expression until they arrive at a new steady state. Each network of genes can behave in different ways that depend on internal and external cellular conditions. In this paper, we consider, for a given network, an entire collection of a particular type of models (monotone Boolean models) that represent all different ways that the network can behave. Then, for any given state a network can potentially be in, we describe all monotone Boolean models that have that state as a steady state. We consider those states that are

Data availability statement: The code used to generate the Figures and Tables are in the following public depositories: https://doi.org/10.5281/zenodo.18682834 https://github.com/Harshavardhan-BV/Monotone-Bool-Net.

Funding: This work was supported by the Prime Minister's Research Fellowship (PMRF), (to HBV), Param Hansa Philanthropies (to MKJ) and the National Science Foundation (DMS-1951510 to TG). The funders had no role in study design, data collection and analysis, decision to publish, or preparation of the manuscript.

Competing interests: The authors have declared that no competing interests exist.

supported by more models to be more likely to represent the states that the network will be in. We apply our approach to the EMT network, which is important in cancer metastasis. We show that the most common steady states correspond to epithelial and mesenchymal states, and that the bistability between these two states is the most common bistability. This confirms the experimental results that these are the most common states of the EMT network.

1 Introduction

Unicellular organisms and cells in multicellular organisms solve complicated control problems related to the allocation of resources, division, and many others quickly and efficiently. Most of these tasks involve activation, deactivation, or expression of new proteins. The main conceptual model of how the chemical signal results in these changes takes the form of a *network* of directed interactions, where the presence of one signal results in increased or decreased activity/abundance of a downstream signal.

Many regulatory networks have been constructed [1–8] for organisms and tasks ranging from *Escherichia coli* to humans. An important question with obvious biological implications is to understand the range of dynamics a given network can support. In particular, a first step is to describe the steady states the network can support, as these are interpreted as different phenotypes that the network can support.

Experimentally, this is an untractable question, since the answer depends on both the external conditions and the internal state of the cell. Using mathematical models to answer this question is difficult, as the answer may depend on the choice of a model, its parameterization, and the choice of an initial condition. Unknown parameters can be addressed using parameter sampling methods [9] or using combinatorial parameterization of all ODE models with steep nonlinearities [10,11], but both of these approaches quickly approach their limits when dealing with large networks. An alternative modeling approach of using a Boolean network model [12–15] has the (apparent) advantage of not needing any parameters, but the choice of update functions is a form of parameterization. Often, these models analyze a single, or only a few, Boolean models compatible with the network, raising the question of whether some potential dynamics have been missed.

We propose a different approach [16] by constructing a finite collection of all monotone Boolean models (MBM) compatible with the network [17]. This includes monotone Boolean models whose influence graph is a strict subgraph of the directed graph of the network.These are constructed as collections of monotone Boolean functions [18] (MBF) that update the state of each node based on its inputs. The monotonicity of the Boolean function reflects the network activation vs. deactivation edges. Monotone Boolean functions can be constructed by induction, but their size grows rapidly [19,20]. In this approach, the network dynamics is a collection of all dynamics supported by all monotone Boolean models, which is weighted in

importance by its prevalence. That is, if a particular steady state is supported by 80% of all MBMs, then it is more important than a steady state that is only supported by 10% of all MBMs.

Since the number of MBMs for a given network is finite, the prevalence of all dynamics is, in principle, computable. However, the number of MBM grows very quickly, and even computing steady states for a single MBM is NP-complete [21–23].

In this paper, we concentrate on *balanced strongly connected networks*, which are networks that have no negative loops (cycles) and there is a directed path between any two nodes. We show that for such networks, the MBMs that support particular equilibria have a structure of products of down- and up-sets in lattices of MBFs. As a result of this characterization, we are able to completely describe the prevalence of each Boolean steady state, bistability, and multistability for any such network. This leads to a general computational procedure that we illustrate on monotone Boolean functions with $k = 1,2,3$ inputs, MBF(k), and several monotone Boolean models comprised of such MBFs.

We start by showing that there is a change of variables that results in a one-to-one correspondence between monotone Boolean models for any balanced network [24,25] and monotone Boolean models compatible with networks with all activating edges (positive networks). We then analyze positive networks and use the change of variables to obtain results for the original balanced networks. Balanced directed signed graphs (networks) are closely related to *balanced* undirected signed graphs. Balanced signed graphs are important in many areas of science [26–28]. In fact, in strongly connected signed directed graphs, every undirected cycle is positive if every directed cycle is [29]. Therefore, for balanced directed networks, considered in this paper, the underlying undirected signed graph is also balanced.

After illustrating our approach on a toggle switch network, we consider networks with a 2-team network structure, which were recently described [30,31]. Here, edges connecting the nodes from the same team are activating, but those connecting nodes from opposite teams are repressing. We show that such networks are balanced and that the most prevalent phenotypes are those where one team is active, while the other is not, and the most prevalent bistability is between these two phenotypes.

We then study two EMT networks: one a six-node network [1] and one with 15 nodes and 59 edges [2]. We show that the most prevalent states supported by both networks are the epithelial and mesenchymal states, and that bistability between them is the most prevalent bistability. This work also allows studying the prevalence of other steady states apart from mesenchymal and epithelial states, which are linked with the discussion about so-called *intermediate steady states*, which have biological significance [32].

The paper is organized as follows: After introducing basic definitions, we discuss balanced networks in section *balanced networks*. The main result of this section is that all monotone Boolean models of a balanced network are in one-to-one correspondence with monotone Boolean models of a positive network. In section *Steady states for positive MBMs*, we characterize MBMs that support a particular steady state, and in sections *Bistability* and *Multistability*, those that support bistability and multistability, respectively. We illustrate our results throughout the text on several networks, including toggle switch, toggle switch with self-loops, 2-team network, and two EMT network models with 6 and 15 nodes. In the *Methods* section, we use lattice theory to describe the sets of MBF, which we use to construct MBMs that support steady states. We close the paper with a discussion.

2 Results

Definition 2.1. *A regulatory network* $RN = (V, E, \delta)$ *is a directed graph* $G = (V,E)$ *with nodes* V *with* $|V| = N$*, directed edges* E*, and an edge sign function* $\delta : E \to \{-1, 1\}$*. We denote an edge from node* v_i *to node* v_j *without indicating its sign by* (v_i, v_j) *or* $v_i \multimap v_j$*. The edge* $v_i \multimap v_j$ *is activating if* $\delta(v_i, v_j) = 1$ *and repressing if* $\delta(v_i, v_j) = -1$*. Graphically, an activating edge of a regulatory network edge is denoted by* $v_i \to v_j$ *and a repressing edge by* $v_i \dashv v_j$*. The sources and targets of a node* v_i *are given by*

$$\mathbf{S}(v_i) := \{v_k \in V \mid v_k \multimap v_i \in E\} \text{ and } \mathbf{T}(v_i) := \{v_j \in V \mid v_i \multimap v_j \in E\},$$

respectively. In addition, we assume that the directed graph is strongly connected and so there is a directed path between any two nodes.

Definition 2.2. *A loop in network RN is a set of edges* $(v_1, v_2), (v_2, v_3), \ldots, (v_k, v_{k+1})$ *with* $v_1 = v_{k+1}$. *A loop is positive (negative) if the product of the signs of edges*

$$\prod_{i=1}^{k} \delta(v_i, v_{i+1})$$

is 1 (–1).

Definition 2.3. *A regulatory network* $RN = (V, E, \delta)$ *is balanced if it has no negative loops.*

Definition 2.4. *A Boolean function* $f\colon \mathbb{B}^k \to \mathbb{B}$ *is increasing with respect to input j if for any input* $b = (b_1, \ldots, b_k) \in \mathbb{B}^k$

$$f(b_1, \ldots, b_{j-1}, 0, b_{j+1}, \ldots, b_k) \leq f(b_1 \ldots, b_{j-1}, 1, b_{j+1}, \ldots, b_k).$$

It is strictly increasing with respect to *j if there is at least one input* $b \in \mathbb{B}^N$ *where the inequality is strict.*

A Boolean function $f\colon \mathbb{B}^k \to \mathbb{B}$ *is decreasing with respect to input j if for any collection of* $b_i \in \mathbb{B}$

$$f(b_1, \ldots, b_{j-1}, 0, b_{j+1}, \ldots, b_k) \geq f(b_1, \ldots, b_{j-1}, 1, b_{j+1}, \ldots, b_k).$$

It is strictly decreasing with respect to *j if there is at least one input* $b \in \mathbb{B}^k$ *where the inequality is strict.*

Definition 2.5. *A Boolean function* $f\colon \mathbb{B}^k \to \mathbb{B}$ *is monotone if it is increasing or decreasing with respect to each input* $i = 1, \ldots, k$. *In this case, f is called a* monotone Boolean function.

A set of increasing monotone Boolean functions $f\colon \mathbb{B}^k \to \mathbb{B}$ will be denoted by $MBF(k)$.

In Fig 1a, we show three increasing monotone Boolean functions $MBF(1)$ with a single input denoted X. These are the zero function **0**, the identity function *Id*, and the one function **1**. We represent these three functions as nodes, connected by edges if their truth values differ on a single input string. In Fig 1b we list six increasing monotone Boolean functions $MBF(2)$ with two inputs denoted X and Y. Their names are in the top row of the table; function X copies the values of the

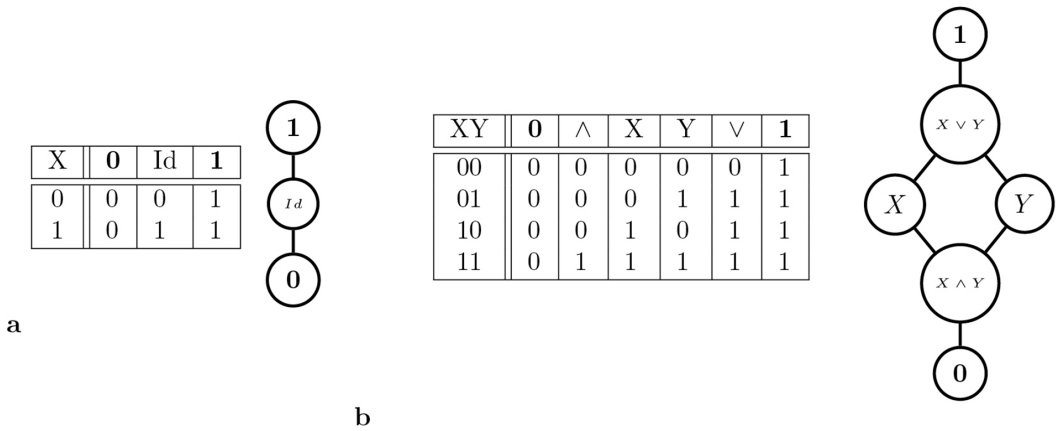

X	**0**	Id	**1**
0	0	0	1
1	0	1	1

a

XY	**0**	∧	X	Y	∨	**1**
00	0	0	0	0	0	1
01	0	0	0	1	1	1
10	0	0	1	0	1	1
11	0	1	1	1	1	1

b

Fig 1. (a) There are three monotone Boolean functions with single input *MBF*(1) and (b) six monotone Boolean functions with 2 inputs *MBF*(2).

https://doi.org/10.1371/journal.pcsy.0000103.g001

input X, while the function Y copies the input Y. Similarly, we represent these functions in the form of a graph where again, nodes are connected by edges if their truth values differ on a single input string.

As we will see in section 3.1, the sets $MBF(k)$ for any k form a mathematical structure called *lattice*. The language and results from lattice theory will help in understanding which Boolean models support which steady states.

We now discuss monotone Boolean models of network dynamics $f = (f_1, \ldots, f_N)$ where the update function f_i at the node v_i is a monotone Boolean function.

Definition 2.6. *A Boolean model* $f\colon \mathbb{B}^N \to \mathbb{B}^N$, $f = (f_1, \ldots, f_N)$, *is monotone if for every i the function* f_i *is monotone.*

A Boolean model $f\colon \mathbb{B}^N \to \mathbb{B}^N$ *is positive if for every i the function* f_i *is monotone increasing.*

Definition 2.7. *An influence graph* $I_f = (V, \hat{E})$ *of a monotone Boolean model* $f\colon \mathbb{B}^N \to \mathbb{B}^N$ *is a directed graph with nodes* $v_i, i \in \{1, \ldots, N\}$ *for each variable and a directed edge* $v_j \to v_i$ *if, and only if,* f_i *is strictly increasing or strictly decreasing with respect to j.*

Since our definition of monotonicity is not strict, for a given regulatory network RN with directed graph $G=(V,E)$ we consider a monotone Boolean model f to be a valid model of network dynamics if its influence network $I_f \subset G$ is a subnetwork of the directed graph G. Since the vertex set of I_f and G is the same, this is equivalent to the inclusion of the edges $\hat{E} \subset E$. The inclusion of the functions f with $\hat{E} \subsetneq E$ makes $MBF(k)$ a lattice. This, in turn, allows a compact description of sets of functions that support a particular fixed point.

2.1 Balanced networks

Consider a monotone Boolean model $f = (f_1, \ldots, f_N)$, where each $f_i\colon \mathbb{B}^{k_i} \to \mathbb{B}$. Apply a change of variables $\alpha = (\alpha_1, \ldots, \alpha_N)$ where for each i either $\alpha_i(x_i) = x_i$ or $\alpha_i(x_i) = \neg x_i$. Let $E \subset \{1, \ldots, N\}$ be the indices i where $\alpha_i(x_i) = x_i$.

Then for any $i = 1, \ldots, N$

$$j \in E \implies f_i \text{ is increasing (decreasing) in } x_j \leftrightarrow f_i \text{ is increasing (decreasing) in } \alpha_j(x_j)$$
$$j \notin E \implies f_i \text{ is increasing (decreasing) in } x_j \leftrightarrow f_i \text{ is decreasing (increasing) in } \alpha_j(x_j)$$

Then

$$i \in E \implies f_i \text{ is increasing (decreasing) in } x_j \leftrightarrow f_i \text{ is increasing (decreasing) in } \alpha_i(x_j)$$
$$i \notin E_i \implies f_i \text{ is increasing (decreasing) in } x_j \leftrightarrow f_i \text{ is decreasing (increasing) in } \alpha_i(x_j)$$

On the other hand, applying the negation operation to the function f_i, we get

$$f_i \text{ is increasing (decreasing) in } x_j \leftrightarrow \neg f_i \text{ is decreasing (increasing) in } x_j$$

We have the following Theorem.

Theorem 2.8. *Consider a balanced network RN and a monotone Boolean model* $f = (f_1, \ldots, f_N)$ *compatible with RN. Then there is a change of variables* $\alpha : \mathbb{B}^N \to \mathbb{B}^N$ *with* $\alpha \circ \alpha = Id$*, and a positive Boolean model* $g = (g_1, \ldots, g_N)$ *such that the following diagram commutes*

$$\begin{array}{ccc} \mathbb{B}^N & \xrightarrow{f} & \mathbb{B}^N \\ {\scriptstyle\alpha}\uparrow\downarrow{\scriptstyle\alpha} & & {\scriptstyle\alpha}\uparrow\downarrow{\scriptstyle\alpha} \\ \mathbb{B}^N & \xrightarrow{g} & \mathbb{B}^N \end{array}$$

Proof can be found in section 3.1.

Note that the commutative diagram above implies that any trajectory under f, say

$$x_t = f(x_{t-1}), x_{t-1} = f(x_{t-2}) \ldots, x_1 = f(x_0)$$

exists if, and only if there is a corresponding trajectory under g

$$\alpha(x)_t = g(\alpha(x)_{t-1}), \alpha(x)_{t-1} = g(\alpha(x)_{t-2}) \ldots, \alpha(x)_1 = g(\alpha(x)_0).$$

In particular, x is a fixed point under f, if, and only if $\alpha(x)$ is a fixed point under g

$$x = f(x) \iff \alpha(x) = g(\alpha(x)).$$

This shows that every balanced network has the same dynamics as a positive network, where all edges are positive. Since an MBM $f = (f_1, \ldots, f_N)$ for a network with all positive edges has all functions f_i that are increasing MBFs, it is sufficient to study steady states and multistability for positive networks.

We illustrate the change of variables in Fig 2.

In Fig 2a is a toggle switch [33], one of the basic network examples. Using Theorem 2.8, note that the map $\alpha(A, B) = (\neg A, B)$ results in both $g_B(A)$ and $g_A(B)$ to be increasing. Thus $\alpha = (\neg A, B)$ transforms f to a positive Boolean model g (Fig 2a). The change of variables α is not unique; it is easy to see that $\alpha = (A, \neg B)$ also transforms f to a positive

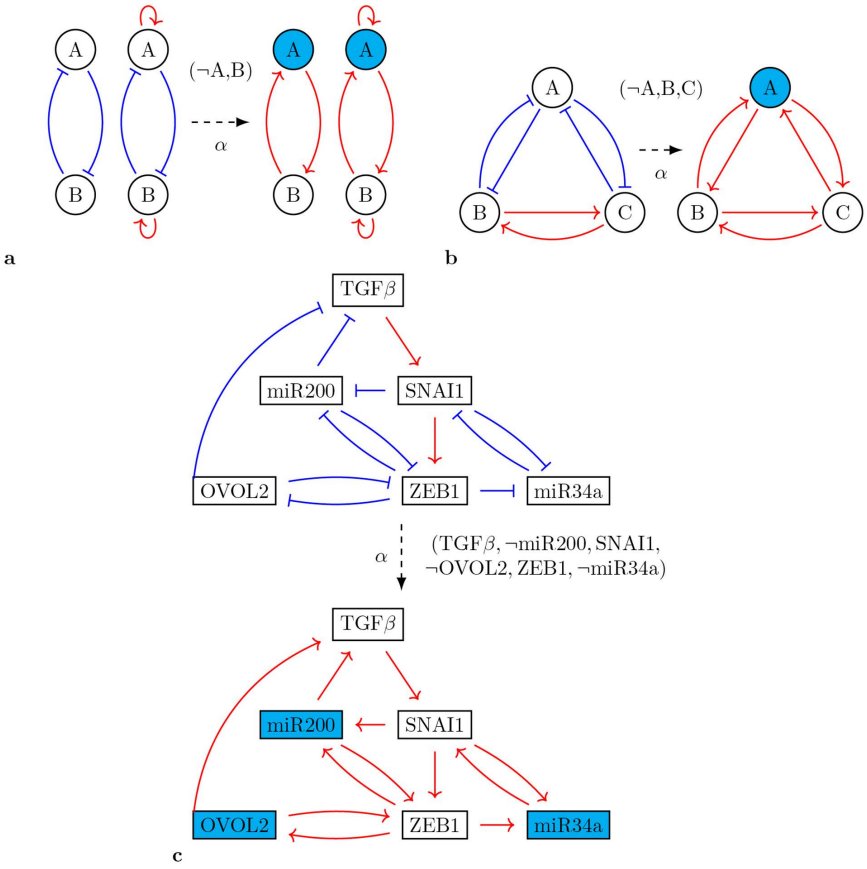

Fig 2. Schematic representation of the change of variables to obtain a positive network. The cyan nodes represent the nodes that have ¬ in α. **(a)**: Toggle switch (left: without self-regulation, right: with self-activation), **(b)**: 2-team network with 3 nodes, and **(c)**: EMT network.

https://doi.org/10.1371/journal.pcsy.0000103.g002

Boolean model g. Similarly, a toggle switch with self-activations can be transformed into a positive Boolean model using the same transformation.

In Fig 2b we consider a toy example of a 2-team network, studied in [34]. We define a 2-team network as a network where the set of nodes V can be decomposed into two disjoint sets A and B, $V = A \cup B$, in such a way that the nodes of the same team activate each other while inhibiting the nodes of the opposite team. In other words, $v_i \to v_j$ if, and only if, $v_i, v_j \in A$, or $v_i, v_j \in B$, and $v_i \dashv v_j$, if, and only if $v_i \in A, v_j \in B$, or $v_i \in B, v_j \in A$.

Here node A belongs to one team, whereas B and C belong to the other team. It is easy to see that transformation $\alpha = (\neg A, B, C)$, or transformation $\alpha = (A, \neg B, \neg C)$ transforms f into a positive Boolean model g (Fig 2b).

Finally, we consider the biologically important *EMT* network which governs epithelial-to-mesenchymal transition (EMT) [1,35], where we do not consider the input and output nodes from the original network and exclude the self-inhibition present on SNAI1. Then α = (TGF β, ¬miR200, SNAI1, ¬OVOL2, ZEB1, ¬miR34a) transforms f into a positive model g (Fig 2c).

2.2 Steady states for positive MBMs

We are now ready to address the main question posed in this paper: *How many MBMs compatible with a balanced network support a particular steady state?*

Because of Theorem 2.8, it is sufficient to address this question only for positive monotone Boolean models. To this end, we define the following sets

Definition 2.9. *Consider the set MBF(k), a set of monotone Boolean functions* $f : \mathbb{B}^k \to \mathbb{B}$. *For any input* $b \in \mathbb{B}^k$ *let*

$$U(b) := \{f \in MBF(k) \mid f(b) = 1\}$$
$$L(b) := \{f \in MBF(k) \mid f(b) = 0\}.$$

In other words, U(b) (L(b)) is the set of functions that evaluate to 1 (0). As an illustration, we show these intervals for the set MBF(2) of positive monotone Boolean functions (see Fig 1b) and Table 1.

We are ready for the main result.

Theorem 2.10. *Consider a positive network RN and an arbitrary Boolean state* $e = (e_1, \ldots, e_N) \in \mathbb{B}^N$ *of the network RN. Then e is a steady state of any monotone Boolean model* $f = (f_1, f_2, \ldots, f_N)$ *where*

$$f_i \in Z_i(e)$$

where

$$Z_i(e) = \begin{cases} U(e_{\mathbf{s}(i)}) & \text{if} \quad e_i = 1 \\ L(e_{\mathbf{s}(i)}) & \text{if} \quad e_i = 0 \end{cases}$$

where $e_{\mathbf{s}(i)}$ *are the values of the input nodes of* v_i *evaluated at the state e.*

Table 1. Sets of functions in MBF(2) that evaluate to 0 (left) and 1 (right). The third column in each part lists the number of functions in the corresponding set.

L(11)	**{0}**	**1**	**U(11)**	{**1**, $X \vee Y, X, Y, X \wedge Y$}	**5**
L(10)	{**0**, $X \wedge Y, Y$}	3	U(10)	{**1**, $X \vee Y, X$}	3
L(01)	{**0**, $X \wedge Y, X$}	3	U(01)	{**1**, $X \vee Y, Y$}	3
L(00)	{**0**, $X \wedge Y, X, Y, X \vee Y$}	5	U(00)	{**1**}	1

https://doi.org/10.1371/journal.pcsy.0000103.t001

Proof. Vector $e \in \mathbb{B}^N$ is an equilibrium under a monotone Boolean model $f = (f_1, \ldots, f_N)$ where $f_i \in MBF(|\mathbf{S}(i)|)$ if and only if

$$e_i = f_i(e_{\mathbf{S}(i)}).$$

That is, f_i evaluated on the values of e restricted to sources of node i evaluates to the value e_i. Since $U(e_{\mathbf{S}(i)}) \subset MBF(|\mathbf{S}(i)|)$ is the set of functions that evaluate to 1 on input $e_{\mathbf{S}(i)}$ and $L(e_{\mathbf{S}(i)}) \subset MBF(|\mathbf{S}(i)|)$ is the set of functions that evaluate to 0 on input $e_{\mathbf{S}(i)}$, the result follows.

In the section 3.1 we show that the sets U are ideals (down-sets) and filters (up-sets) in lattices. In addition, we show there the following characterization of the largest set U and the largest set L.

Lemma 2.11.

- *The largest set $U \subset MBF(k)$ is the set $U(\mathbb{1}_k)$ where $\mathbb{1}_k$ is the vector of ones of length k, with $|U(\mathbb{1}_k)| = |MBF(k)| - 1$*
- *the largest set $L \subset MBF(k)$ is the set $L(\mathbb{0}_k)$ where $\mathbb{0}_k$ is the vector of zeros of length k, with $|L(\mathbb{0}_k)| = |MBF(k)| - 1$.*

Proof can be found in section 3.1.

The next corollary of Lemma 2.11 characterizes the equilibria that are supported by most monotone Boolean models.

Theorem 2.12. *Consider a positive network RN with N nodes. Then*

- *Every state in $\mathbb{B}^N$ is an equilibrium for some monotone Boolean model.*
- *For positive network RN with N among all the states, the states $\mathbb{0} \in \mathbb{B}^N$ and $\mathbb{1} \in \mathbb{B}^N$ are most prevalent, i.e., supported by most MBMs. The set of all MB models compatible with RN is*

$$MBM := MBF(k_1) \times MBF(k_2) \times \ldots MBF(k_N),$$

where $k_j = |\mathbf{S}(v_j)|$.

- *The sets of MBMs that supports $\mathbb{0} \in \mathbb{B}^N$ has the form*

$$L(\mathbb{0}_{k_1}) \times L(\mathbb{0}_{k_2}) \times \ldots L(\mathbb{0}_{k_N}),$$

which has the size

$$(|MBF(k_1)| - 1) \times (|MBF(k_2)| - 1) \times \ldots (|MBF(k_N)| - 1). \tag{1}$$

- *The sets of MBMs that supports $\mathbb{1} \in \mathbb{B}^N$ has the form*

$$U(\mathbb{1}_{k_1}) \times U(\mathbb{1}_{k_2}) \times \ldots U(\mathbb{1}_{k_N}).$$

which also has the size (1).

Proof can be found in section 3.1.

Remark 2.13. *The first conclusion of Theorem 2.12 crucially depends on our choice to consider non-strict definition of monotonicity, since the class of monotone Boolean functions always includes constant functions and any fixed point is supported by at least a set of constant functions with the values matching components of the fixed point.*

We are now ready to apply the theory to the examples in Fig 2. In the toggle switch, the change of variables α allows us to look at the equivalent problem of equilibria in a positive toggle switch where both edges are positive. Since each node has a single input, the set of MBMs f has the form $f=(f_1,f_2)$ with $f_i \in MBF(1)$. Therefore there are $3\times 3=9$ monotone Boolean models $f=(f_1,f_2)$, see Fig 1a for MBF(1) and Fig 3a for the set of models. It is easy to see that

$$U(1) = \{\mathbf{1}, Id\}, \quad U(0) = \{\mathbf{1}\}, \quad L(0) = \{\mathbf{0}, Id\}, \quad L(1) = \{\mathbf{0}\}.$$

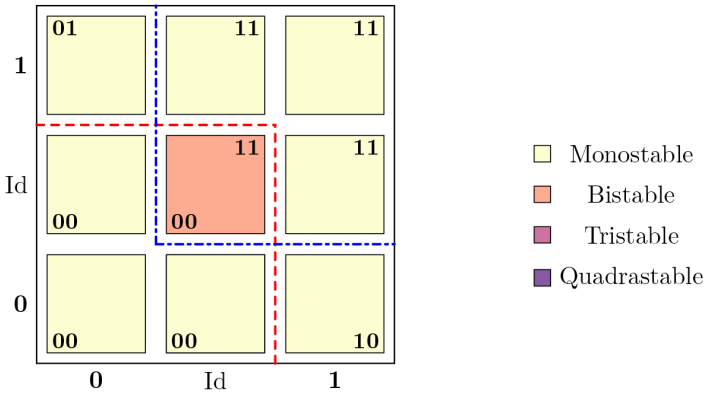

a

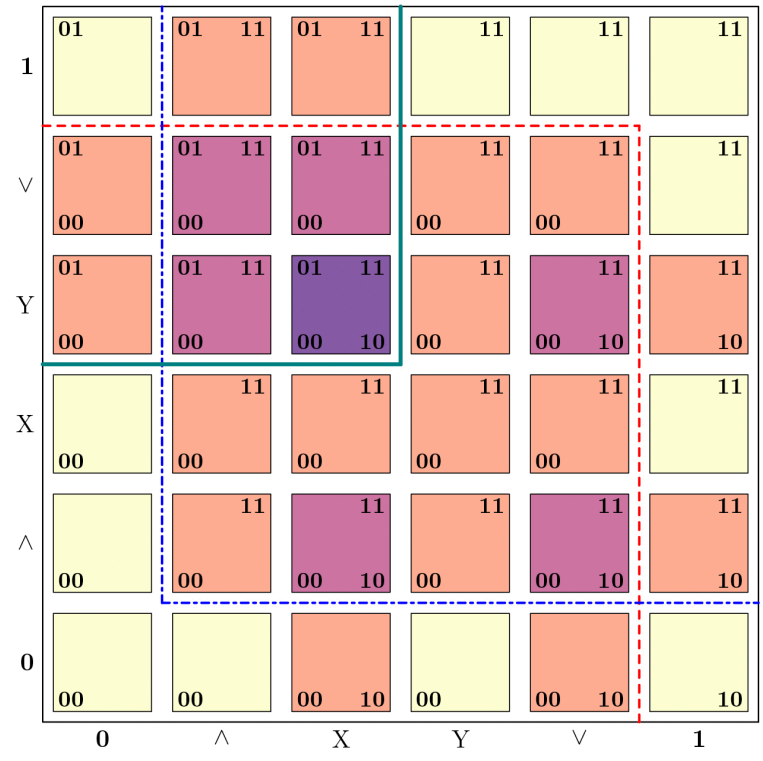

b

Fig 3. Parameter graphs (f_1, f_2) and the steady states supported by (a):$MBF(1)\times MBF(1)$ and (b):$MBF(2)\times MBF(2)$. The states supported are denoted in each square. The red dashed line, blue dash-dotted line, and the teal bold line delineate the set of models that support the steady states (00), (11), and (01), respectively. The filled colors represent the type of exact multistability supported by the corresponding Boolean model $f=(f_1, f_2)$.

https://doi.org/10.1371/journal.pcsy.0000103.g003

Therefore

- steady state (00) is supported by $f \in L(0) \times L(0)$ which has 4 models;
- steady state (10) is supported by $f \in U(0) \times L(1)$ which has 1 model;
- steady state (01) is supported by $f \in L(1) \times U(0)$ which has 1 model;
- steady state (11) is supported by $f \in U(1) \times U(1)$ which has 4 models.

Applying the change of variable function $\alpha : \mathbb{B}^2 \to \mathbb{B}^2$ of the form $(A, B) \to (\neg A, B)$ to the equilibria set in this list, we have the following result for the toggle switch

- steady state (10) is supported by 4 models;
- steady state (00) is supported by 1 model;
- steady state (11) is supported by 1 model;
- steady state (01) is supported by 4 models.

For the toggle switch with self-activation, the same change of variables α as in the toggle switch changes the model to $g = (g_1, g_2)$ where each $g_i \in MBF(2)$ has two inputs, see Fig 1b The set of MBMs has $6 \times 6 = 36$ models, see Fig 3b for the set of models and Table 1 for the list of intervals $U(b), L(b) \subset MBF(2)$. The dominant steady states are the same as in the toggle switch network, but they are supported by a larger number of models:

- steady state (00) is supported by $f \in L(00) \times L(00)$ which has $5 \times 5 = 25$ models;
- steady state (11) is supported by $f \in U(11) \times U(11)$ which also has $5 \times 5 = 25$ models.

After applying α, the most prevalent steady states in the toggle switch with self-activation are

- steady state (10) supported by 25 models;
- steady state (01) supported by 25 models.

For the 2-team network in Fig 2b, any MBM $f = (f_1, f_2, f_3)$ can be changed to $g = (g_1, g_2, g_3)$ with $g_i \in MBF(2)$. Again, all states are supported by some models, but the most prevalent steady states are

- steady state (000) is supported by $f \in L(00) \times L(00) \times L(00)$ which has $5^3 = 125$ models;
- steady state (111) is supported by $f \in U(11) \times U(11) \times U(11)$ which also has $5^3 = 125$ models.

Applying $\alpha : \mathbb{B}^3 \to \mathbb{B}^3$, $\alpha = (A, B, C) \to (\neg A, B, C)$, gives the most common steady states as

- (100) supported by 125 models;
- (011) supported by 125 models.

Finally, for the EMT network in Fig 2c the change of variables

$$\alpha = (TGF\beta, \neg miR200, SNAI1, \neg OVOL2, ZEB1, \neg miR34a)$$

transforms f into a positive model g (Fig 2c). The collection of MBMs $f = (f_\beta, f_{200}, f_S, f_O, f_Z, f_{34})$ for the positive EMT (P-EMT) network is

$$f \in MBF(2) \times MBF(2) \times MBF(2) \times MBF(1) \times MBF(3) \times MBF(2),$$

where the numbers correspond to the number of inputs of the corresponding nodes. The collection *MBF*(3) is shown in Fig 6 and has 20 functions. Therefore, there is a total of

$$6 \times 6 \times 6 \times 3 \times 20 \times 6 = 77760 \quad \text{models.}$$

Within this collection of MBMs, the most common steady states are

- (111111) which is supported by models in $5 \times 5 \times 5 \times 2 \times 19 \times 5 = 23750$ models;
- (000000) which is also supported by 23750 models.

Applying the change of variables α, it follows that the most common steady states in the original EMT network are states

$$(101010) \qquad \text{and} \qquad (010101),$$

each of which is supported by 23750 out of 77760 MBMs compatible with the EMT network. These two states represent the mesenchymal and epithelial state, respectively, with the mesenchymal state characterized by TGFβ, SNAI1, and ZEB1 high, whereas the epithelial state is characterized by miR200, OVOL2, and miR34a high.

Similarly, Theorem 2.10 can be used to calculate the number of MBMs supporting the other states for the positive network, as given in Table 2. These states correspond to the intermediate states characterized by mixed expression of the canonical epithelial and mesenchymal markers.

Consider now a larger EMT network in Fig 4, described in [2], with 15 nodes and 59 edges (excluding the input/output nodes and self-inhibitions). The description of sets $L(\cdot)$, $U(\cdot)$ becomes computationally challenging due to nodes like ZEB1 and ZEB2 having many inputs (12 and 10, respectively). However, leveraging Theorem 2.12 allows identification of the most common states by transforming the most common states $\mathfrak{o}$ and $\mathfrak{1}$ of the positive network using α. It can be seen that this network is balanced, and there exists α given by:

$$\alpha = (TGF\beta, ZEB1, ZEB2, SNAI1, SNAI2, FOXC2, TWIST1, TWIST2, GSC, \neg miR141, \neg miR100, \neg miR34a, \neg miR200a, \neg miR200b, \neg miR200c)$$

Therefore the most common states in the network in Fig 4 are (1) TGFβ, ZEB1, ZEB2, SNAI1, SNAI2, FOXC2, TWIST1, TWIST2, GSC high and miR141, miR100, miR34a, miR200a, miR200b, miR200c low, which corresponds to the mesenchymal state and (2) the state where the first group of nodes are low and the second group is high, which corresponds to the epithelial state. This mathematical result supports the biological insight that the main role of this model is to modulate the transition between these two states. At the same time, the fact that the most prevalent states in the MB models are indeed the epithelial and mesenchymal states supports the idea that looking for the most prevalent states in MB models of a network may reveal the biological significance of the network.

2.3 Bistability

As we have shown in Theorem 2.12, the most common equilibria in any balanced network have the same abundance. A natural question arises whether the bistability between these two equilibria is also the most common form of bistability. Note that in our work, we will refer to the presence of two or more steady states by the term *bistability*. We will use the term *exact bistability* for the presence of exactly two steady states. Specifically, when we say that a model supports bistability between states *d* and *e*, we mean that *d* and *e* are among the steady states, but other steady states beyond *d* and *e* may also exist.

The following theorem extends Theorem 2.10 by characterizing the MBMs that support a bistability between two steady states in the set of positive MBMs.

Table 2. Number of models supporting the top 12 most common steady states. P-EMT-state represents the state in the positive EMT network and EMT state represents the state in the original network after transformation. Calculations we done with code included in depository [36].

P-EMT state	Parameter sets	No. of MBMs	EMT state
(000000)	$L(00) \times L(00) \times L(00) \times L(0) \times L(000) \times L(00)$	23750	(010101)
(111111)	$U(11) \times U(11) \times U(11) \times U(1) \times U(111) \times U(11)$	23750	(101010)
(000100)	$L(01) \times L(00) \times L(00) \times U(0) \times L(001) \times L(00)$	5250	(010001)
(111011)	$U(10) \times U(11) \times U(11) \times L(1) \times U(110) \times U(11)$	5250	(101110)
(001001)	$L(00) \times L(10) \times U(01) \times L(0) \times L(010) \times U(10)$	3780	(011100)
(110110)	$U(11) \times U(01) \times L(10) \times U(1) \times U(101) \times L(01)$	3780	(100011)
(100100)	$U(01) \times L(00) \times L(10) \times U(0) \times L(001) \times L(00)$	3150	(110001)
(011011)	$L(10) \times U(11) \times U(01) \times L(1) \times U(110) \times U(11)$	3150	(001110)
(000001)	$L(00) \times L(00) \times L(01) \times L(0) \times L(000) \times U(00)$	2850	(010100)
(111110)	$U(11) \times U(11) \times U(10) \times U(1) \times U(111) \times L(11)$	2850	(101011)
(100000)	$U(00) \times L(00) \times L(10) \times L(0) \times L(000) \times L(00)$	2850	(110101)
(011111)	$L(11) \times U(11) \times U(01) \times U(1) \times U(111) \times U(11)$	2850	(001010)

https://doi.org/10.1371/journal.pcsy.0000103.t002

Theorem 2.14. *Consider a positive network RN and two arbitrary Boolean states* $d, e \in \mathbb{B}^N$. *Then the bistability between steady states d and e is supported by any positive monotone Boolean model* $f = (f_1, f_2, \ldots, f_N)$ *where*

$$f_i \in Z_i(d) \cap Z_i'(e)$$

where

$$Z_i(d) = \begin{cases} U(d_{\mathbf{s}(i)}) & \text{if} \quad d_i = 1 \\ L(d_{\mathbf{s}(i)}) & \text{if} \quad d_i = 0 \end{cases}$$

and

$$Z_i'(e) = \begin{cases} U(e_{\mathbf{s}(i)}) & \text{if} \quad e_i = 1 \\ L(e_{\mathbf{s}(i)}) & \text{if} \quad e_i = 0 \end{cases}$$

where $d_{\mathbf{s}(i)}, (e_{\mathbf{s}(i)})$ *are the values of the input nodes of* v_i *evaluated at the state d, (e), respectively.*

There are several important consequences of this description. If *i*-th components of *d* and *e* agree, $d_i = e_i$ then

$$Z_i(d) \cap Z_i'(e) \neq \emptyset.$$

However, if $d_i \neq e_i$ then the intersection may be empty. Since *d* and *e* must differ in at least one component, not all pairs of states *d*,*e* can be bistable states for an MBM.

For instance, in the positive toggle switch, the bistability between $d = (00)$ and $e = (11)$ is supported by the set of MBMs $f = (f_1, f_2)$ with

$$f_1 \in L(0) \cap U(1) \quad \text{and} \quad f_2 \in L(0) \cap U(1).$$

These intersections are non-empty and contain a single model

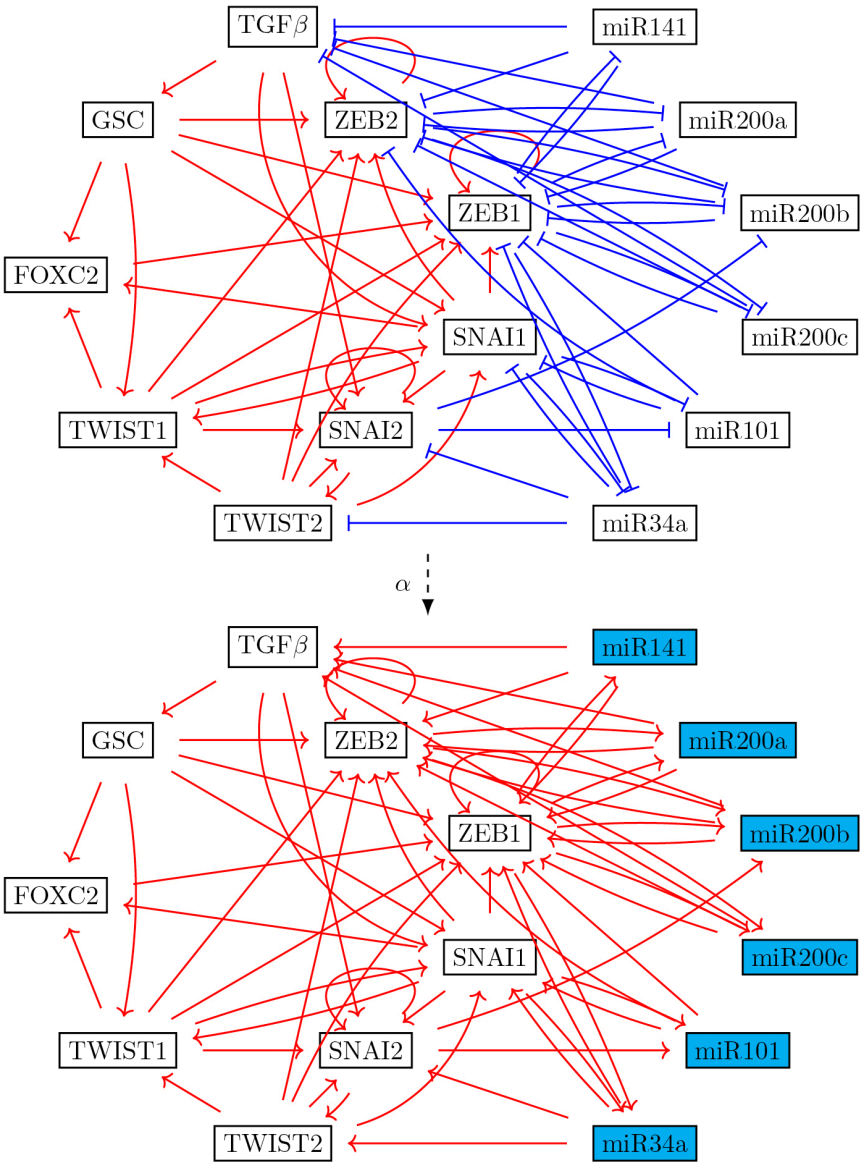

Fig 4. Schematic representation of the change of variables to obtain a positive network of EMT network from [2]. The cyan nodes represent the nodes that have ¬ in α.

https://doi.org/10.1371/journal.pcsy.0000103.g004

$$(f_1, f_2) = (Id, Id),$$

see Fig 3a. This corresponds to a single MBM supporting bistability between (01) and (10) in the toggle switch. However, bistability between (00) and (10) in $MBF(1) \times MBF(1)$ is supported by models $f = (f_1, f_2)$ with

$$f_1 \in L(0) \cap U(0) \quad \text{and} \quad f_2 \in L(0) \cap L(1),$$

where $L(0) \cap U(0) = \emptyset$. Applying the map α, we conclude there are no MBMs for the toggle switch supporting bistability between (10) and (00). In fact, no other pair of states except (01) and (10) can be bistable in a toggle switch, see Fig 3a.

In the case of a toggle switch with self-activation, a larger set of models offers bistability between the states (00) and (11) in the positive network, see Fig 3b. These are the set of MBMs

$$(L(00) \cap U(11)) \times (L(00) \cap U(11)) = 16 \text{ models}$$

Hence, bistability between (01) and (10) is supported by 16 models for the toggle switch with self-activation. However, unlike the toggle switch, bistability between the other pairs of steady states is also supported. The number of models that support these bistabilities in the positive toggle switch are

- (00) and (01): 6 models;
- (00) and (10): 6 models;
- (01) and (11): 6 models;
- (10) and (11): 6 models;
- (01) and (10): 1 model.

We note that while there is only one monotone Boolean model $f = (f_1, f_2) \in MBF(1) \times MBF(1)$ where both functions are strictly increasing with respect to all its inputs (Fig 3a), there are 4 such models

$$(\vee, \vee), (\vee, \wedge), (\wedge, \wedge), (\wedge, \vee) \in MBF(2) \times MBF(2) \qquad \text{(Fig 3b)}.$$

While f supports bistability and one could reasonably argue that only this model represents the true dynamics of the toggle switch, this conclusion is harder to sustain in the larger model. Here, two of the models support bistability and two support tristability; the context provided by the non-strict monotone Boolean models is essential for understanding how these results fit together.

Lemma 2.15. *Consider a positive network RN with N vertices. Then the most common bistability supported by MBMs* $f = (f_1, \ldots, f_N)$ *with*

$$f \in \prod_{i=1}^{N} MBF(k_i)$$

is between the steady states $d = \mathtt{0}$ *and* $e = \mathtt{1}$.

It is supported by

$$\prod_{i=1}^{N} |MBF(k_i)| - 2$$

MBMs.

Proof can be found in section 3.1.

For 2-team network example, Lemma 2.15 shows that the bistability between (100) and (011) is supported by $4^3 = 64$ MBMs, which is $64/216 = 0.296$; or almost 30% of all models.

For the 6-node EMT network, the bistability between epithelial and mesenchymal states is supported by $4 \times 4 \times 4 \times 1 \times 18 \times 4 = 4608$ MBMs. The resulting prevalence is $4608/77760 = 0.059$, or about 6%.

2.4 Multistability

Mirroring our comment about bistability, we will say that an MB model supports q–multistability if it has $n \geq q$ steady states. We will use the term *exact q-multistablity* for MBM that supports exactly q-steady states.

In order to determine the collection of MBMs that support exact q–multistability, it is sufficient to know MBMs that support q–multistability for all $n \geq q$. More precisely, let $m_n(E)$ be the set of MB models that support n–multistability between states $E := \{e_1, \ldots, e_n\}$, for some $n \geq q$, and let $em_q(A)$ be the set of MBMs that support exact q–multistability between states $A = \{e_1, \ldots, e_q\}$. Then

$$em_q(A) = m_q(A) \setminus \bigcup_{n>q, A \subset E} m_n(E).$$

The extension of Theorems 2.10 and 2.14 to multistability is straightforward.

Theorem 2.16. *Consider a positive network RN and q Boolean states $d^1, \ldots, d^q \in \mathbb{B}^N$. Then the multistability between these steady states is supported by any positive monotone Boolean model $f = (f_1, f_2, \ldots, f_N)$ where*

$$f_i \in \bigcap_{j=1}^{q} Z_i(d^j)$$

where

$$Z_i(d^j) = \begin{cases} U(d^j_{\mathbf{S}(i)}) & \text{if} \quad d^j_i = 1 \\ L(d^j_{\mathbf{S}(i)}) & \text{if} \quad d^j_i = 0 \end{cases},$$

where $d^j_{\mathbf{S}(i)}$ are the values of the input nodes of v_i evaluated at the state d^j, respectively.

The conditions under which these products are non-empty are subject to ongoing investigation.

As an example, note that in Fig 3b there is one set of functions (f_1, f_2) that supports multistability between all 4 states (00, 10, 01, 11), 4 models that support tristability between (00, 01, 11) and 4 models that support tristability between (00, 10, 11).

The question of what is the highest multistability supported by the network is related to the number of positive loops in the network, and only partial solutions and estimates are known [37].

3 Methods

3.1 Lattice theory

Definition 3.1 ([38]). *A partially ordered set P (or poset) is a set P together with a binary relation denoted ≤, satisfying the following three axioms:*

1. *For all $t \in P$, $t \leq t$ (reflexivity).*
2. *If $s \leq t$ and $t \leq s$, then $s = t$ (antisymmetry).*
3. *If $s \leq t$ and $t \leq u$, then $s \leq u$ (transitivity).*

We say that two elements s and t of P are comparable if $s \leq t$ or $t \leq s$; otherwise s and t are incomparable, denoted $s \| t$.

Definition 3.2. *A subset D of a poset P is a down-set or order ideal if*

$$x \in D, y \leq x \implies y \in D.$$

We denote the down-sets in P by J(P). Dually, a subset U of P is an up-set or order filter if

$$x \in U, y \geq x \implies y \in U.$$

We denote the up-sets of P by U(P). Since we will only deal with order ideals and order filters, we will shorten these terms to ideal and filter, respectively.

Definition 3.3. *Let P be a poset with two binary operations $\vee$, called join, and $\wedge$, called meet. P is a lattice if every pair of elements of P has both a meet and a join.*

In this paper, we will only consider finite posets and lattices. In a finite lattice, all ideals (filters) are principal [39] and thus have the form

$$\downarrow v := \{x \in \mathcal{L} \mid x \leq v\} \qquad (\uparrow u := \{x \in \mathcal{L} \mid x \geq u\}.$$

Definition 3.4. *Let $\mathcal{L}$ be a lattice.*

1. A nonzero element $j \in \mathcal{L}$ is join-irreducible if j is not the join of two smaller elements, that is, if

$$j = a \vee b \implies j = a \text{ or } j = b.$$

2. Dually, a nonunit element $m \in \mathcal{L}$ is meet-irreducible if m is not the meet of two larger elements, that is, if

$$m = a \wedge b \implies m = a \text{ or } m = b.$$

A subset $A \subsetneq B$ is a *proper* subset of B.

Definition 3.5. ([39]). *Let $\mathcal{L}$ be a lattice.*
A proper ideal J is prime if

$$a \wedge b \in J \implies a \in J \text{ or } b \in J.$$

Dually, a proper filter F is prime if

$$a \vee b \in F \implies a \in F \text{ or } b \in F.$$

Theorem 3.6 (Theorem 3.37, [39]). *The properties of being a prime ideal and being a prime filter are complementary, that is, I is a prime ideal if and only if I^c is a prime filter.*

Definition 3.7 ([39]). *If a lattice $\mathcal{M}$ has a smallest element (which we call 0), and $\mathcal{L}$ is another lattice then the ideal kernel of a lattice homomorphism $f : \mathcal{L} \to \mathcal{M}$ is the set*

$$ker(f) = \{a \mid f(a) = 0\}.$$

This is easily seen to be an ideal of $\mathcal{L}$.

Given a lattice $\mathcal{L}$, choosing $\mathcal{M} = \mathbb{B}$ to be the Boolean lattice $\mathbb{B} := (\{0, 1\}; <)$, we arrive at the concept of the indicator function of a subset $S \subseteq \mathcal{L}$. The *indicator function* of S is the function $f_S : \mathcal{L} \to \mathbb{B}$ defined by setting $f_S(x) = 0$ if and only if $x \in S$. In general, an indicator function need not be a lattice homomorphism. However, the indicator function of a **prime** ideal P is a lattice epimorphism.

Definition 3.8 ([38]). *Lattice $\mathcal{L}$ is a distributive lattice if*

$$s \vee (t \wedge u) = (s \vee t) \wedge (s \vee u)$$
$$s \wedge (t \vee u) = (s \wedge t) \vee (s \wedge u)$$

holds for any elements $s, t, u \in \mathcal{L}$.

The fundamental Theorem for finite distributive lattices is due to Birkhoff [40].

Theorem 3.9 (Birkhoff Theorem). *Any finite distributive lattice is isomorphic to the lattice of down-sets of its join-irreducible elements.*

This representation is crucial for understanding the relationship between join-irreducibles and prime ideals.

Lemma 3.10. *Down set of join-irreducible element in finite distributive lattices are prime ideals.*

Proof. Consider an ideal $(\downarrow v)$. If $x \vee y \in (\downarrow v)$, then by join-irreducibility of v, either $x \leq v$ or $y \leq v$, and therefore that element is also in $\downarrow v$. This directly satisfies the definition of a prime ideal. □

Theorem 3.11 (Theorem 3.41, [39]). *In a lattice* $\mathcal{L}$*, the prime ideals in* $\mathcal{L}$ *are precisely the kernels of the indicator epimorphisms.*

By duality Theorem 3.6, the prime filters are precisely sets U which map to 1 under an indicator epimorphism.

3.2 Lattice of increasing monotone Boolean functions

Consider the poset $\mathbb{B}^k$ of Boolean vectors under the order induced by $0 < 1$ on each component.

The set of increasing monotone Boolean functions $MBF(k)$ is a set of order preserving maps

$$MBF(k) := \{f : \mathbb{B}^k \to \mathbb{B}\}.$$

Definition 3.12 (Truth set and zero set). *The truth set T(f) of a Boolean function* $f : \mathbb{B}^k \to \mathbb{B}$ *is*

$$T(f) := \{b \in \mathbb{B}^k \mid f(b) = 1, \}$$

while the zero set $\ker(f)$ *is*

$$\ker(f) := \{b \in \mathbb{B}^k \mid f(b) = 0.\}$$

Note that $(MBF(k), \preceq)$ is a poset with order given by

$$f \preceq g \quad \Leftrightarrow \quad T(f) \subseteq T(g).$$

Lemma 3.13. *The poset* $(MBF(k), \preceq)$ *is a distributive lattice with operations given by union and intersection of the associated truth sets*

$$\begin{aligned} f \vee g = h \quad &\Longleftrightarrow \quad T(f) \cup T(g) = T(h) \\ f \wedge g = h \quad &\Longleftrightarrow \quad T(f) \cap T(g) = T(h) \end{aligned}$$

Let $G : MBF(k) \to U(P)$ taking $f \to T(f)$

$$G(f) = T(f).$$

The map G is a lattice isomorphism between $(MBF(k), \preceq)$ and $(U(P), \subseteq)$ where we made the orders explicit.

We also define an *anti-order* $\preceq_a$ on $MBF(k)$ by using kernels of the maps f

$$f \preceq_a g \quad \Leftrightarrow \quad \ker f \subsetneq \ker g.$$

It is straightforward to see that

$$f \preceq_a g \quad \Leftrightarrow \quad g \preceq f.$$

Consider a map $F : (MBF(k), \preceq_a) \to J(P)$ taking $f \to \ker f$ and so

$$F(f) = \ker f.$$

Here $J(P)$ is the set of order ideals in P. It is easy to see that the map F is an isomorphism and thus $(MBF(k), \preceq_a) \cong J(P)$.

We have an immediate result.

Lemma 3.14. *$(MBF(k), \preceq_a)$ is a lattice with operations $(\vee_a, \wedge_a)$*

$$f \vee_a g = h \quad \Leftrightarrow \quad f \wedge g = h$$
$$f \wedge_a g = h \quad \Leftrightarrow \quad f \vee g = h$$

where the operations $(\vee, \wedge)$ are operations in lattice $(MBF(k), \preceq)$

We will use notation $MBF(k)$ for $(MBF(k), \preceq)$ and notation MBF^a for lattice $(MBF(k), \preceq_a)$.

Let $S=2^P$ be a set of all subsets of finite poset P. Let

$$\kappa : S \to S, \qquad \kappa(Q) = Q^c \tag{2}$$

which assigns to $Q \in S$ its complement Q^c in S. Then the map κ applied to poset $P := \mathbb{B}^k$ of all possible inputs to $f \in MBF(k)$ maps $T(f)$ to $\ker f$ and $\ker f$ to $T(f)$.

Corollary 3.15. *The map $\kappa : P \to P$ induces an isomorphism between lattices $(MBF(k), \preceq)$ and $(MBF^a(k), \preceq_a)$ which maps meet-irreducible elements to join-irreducible elements and join-irreducible elements to meet-irreducible elements. The isomorphism takes each $f \in MBF(k)$ to itself but exchanges the lattice operations.*

Proof. Since for any two functions $f, g \in MBF(k)$ the union $T(f) \cup T(g)$ is the complement of $\ker f \cap \ker g$ and intersection $T(f) \cap T(g)$ is the complement of $\ker f \cup \ker g$ by de Morgan laws, the result follows from Lemma 3.14.

Recall that in Definition 2.9 we set

$$L(x) = \{f \in MBF(k) \mid f(x) = 0\} \quad \text{and} \quad U(x) = \{f \in MBF(k) \mid f(x) = 1\}.$$

Theorem 3.16. *We have the following characterizations of the sets $L(x), U(x); x \in \mathbb{B}^k$:*

1. *For each x the set L(x) is a prime ideal in MBF(k).*
2. *There is a unique meet-irreducible element $g = g(x) \in MBF(k)$ such that L(x) is a down-set of g in MBF(k), i.e., $L(x) = \downarrow g$.*
3. *For each x the set U(x) is a prime filter in MBF(k)*
4. *There is a unique join-irreducible element $g = g(x) \in MBF(k)$ such that U(x) is an up-set of g in MBF(k), i.e., $U(x) = \uparrow g$.*

Proof. For illustration of the arguments below, please see Fig 5 for MBF(2). The set MBF(3) is shown in Fig 6.

We start by describing all epimorphisms $U(P) \to \mathbb{B}$. First, for every $x \in P$ let

$$u_x : U(P) \to \mathbb{B}$$

be a bounded lattice homomorphism which maps all up-sets of P containing x to 1 and all other up-sets to 0. Note that this set of epimorphisms is in one-to-one correspondence with $x \in P$.

We now show that every lattice epimorphism $f : U(P) \to \mathbb{B}$ has the form u_x for some $x \in P$. Consider any lattice epimorphism $f : U(P) \to \mathbb{B}$. Then the elements $y \in U(P)$ such that $f(y)=0$ that are mapped to 0 must have a unique maximal element $\bar{y}$, which is the join of the elements y that are mapped to 0. This follows from the homomorphism property requiring that if $f(u)=0$ and $f(v) = 0$, then also $f(u \vee v) = 0$. Importantly, $\bar{y}$ must be meet-irreducible, since it cannot be the meet $u \wedge v$ of any elements u,v with $f(u)=f(v) = 1$.

Since $U(P) \cong (MBF(k), \preceq)$ and $J(P) \cong MBF^a(k), \preceq_a)$, the isomorphism from Corollary 3.15 between lattices

$$(MBF(k), \preceq) \qquad \text{and} \qquad (MBF^a(k), \preceq_a)$$

induces isomorphism between $U(P)$ and $J(P)$, By Lemma 3.14 the meet irreducible elements in $U(P)$ are mapped to join-irreducible elements in $J(P)$. Since the isomorphism between $(MBF(k), \preceq)$ and $(MBF^a(k), \preceq_a)$ is induced by κ, it follows from (2) that $\kappa(\bar{y})$ is a join irreducible element of $J(P)$.

We illustrate this map on the example $MBF(2)$ in Fig 5. The set $U(P)$ is depicted in panel Fig 5b and the red nodes correspond to meet-irreducible elements of $U(P)$. Note that $\kappa(\{11, 10, 01\}) = \{00\}$, $\kappa(\{11, 10\}) = \{00, 01\}$, $\kappa(\{11, 01\}) = \{00, 10\}$ and $\kappa(\{\emptyset\}) = P$ and the images are join-irreducible nodes of the lattice $J(P)$ in Fig 5e.

By Lemma 3.10 down-sets of join-irreducible elements in $J(P)$ are prime ideals. Therefore for each $\kappa(\bar{y})$ there exists $\bar{x} \in P$ such that

$$\kappa(\bar{y}) =\downarrow \bar{x}. \tag{3}$$

To summarize our construction so far, for each lattice epimorphism $f : U(P) \to \mathbb{B}$ we associate a meet-irreducible element $\bar{y} \in U(P)$, to which we assign a join-irreducible element $\kappa(\bar{y}) \in J(P)$, which has a form of (3) form some $\bar{x}$. We claim that $f = u_{\bar{x}}$. First, we note that the kernel of the epimorphism f are all the up-sets that are subsets of the largest up-set $\bar{y} \in U(P)$. By construction, the set $\kappa(\bar{y})$ is the complement of the up-set $\bar{y}$ in $S=2^P$ and so it is disjoint from any up-sets in $U(P)$ that are below $\bar{y}$. Furthermore, this complement $\kappa(\bar{y})$ is a prime ideal generated by $\bar{x}$. Therefore, $\bar{x}$ is the largest element in P which does not belong to the upper set $\bar{y}$. As a consequence, if $y \in U(P)$ contains $\bar{x}$, then $f(y)=1$, but if $\bar{x} \notin U(P)$, then $f(y) =0$. This shows that $f = u_{\bar{x}}$.

Therefore, every lattice epimorphism f has the form $f= u_x$ for some x.

Consider $u_x : MBF(k) \to \mathbb{B}$ for some $x \in \mathbb{B}^k$. Then the set of up-sets in P that do not contain x is a down-set in $MBF(k)$ that consists of all functions $f \in MBF(k)$ whose truth set does not contain x, and therefore $f(x)=0$. By definition of the sets $L(x)$, these are precisely the functions that belong to the set $L(x)$. This down-set in $MBF(k)$ is mapped by u_x to 0 and therefore is a kernel of a homomorphism u_x. By Theorem 3.11 $L(x)$ is the kernel of indicator epimorphism and therefore prime ideal in $MBF(k)$. Furthermore there is unique maximal element $\bar{y} \in L(x)$ which is meet -irreducible and such that

$$L(x) =\downarrow \bar{y}.$$

This proves statements 1 and 2 of the Theorem.

We illustrate this in Fig 5c. Down-sets of meet-irreducible elements (in red) are $L(X \vee Y) = L(00), L(Y) = L(01), L(X) = L(10), L(\mathbf{0}) = L(11)$. At the same time $L(11) = \ker u_{00} = \{\mathbf{0}\}$, $L(10) = \ker u_{01} = \{\mathbf{0}, X \wedge Y, X\}$, $L(01) = \ker u_{10} = \{\mathbf{0}, X \wedge Y, Y\}$ and $L(00) = \ker u_{11} = \{\mathbf{0}, X \wedge Y, X, Y, X \vee Y\}$.

By Theorem 3.6 the complements of prime ideals are prime filters. This shows $U(x)$ are upsets of join-irreducible elements which proves 3 and 4.

To illustrate, note that in Fig 5f the down-sets of meet-irreducible elements in $MBF^a(2)$ (in red), which are upsets of join-irreducibles in $MBF(2)$, are $U(X \wedge Y) = U(11), U(Y) = U(01), U(X) = U(10), U(\mathbf{1}) = U(00)$.

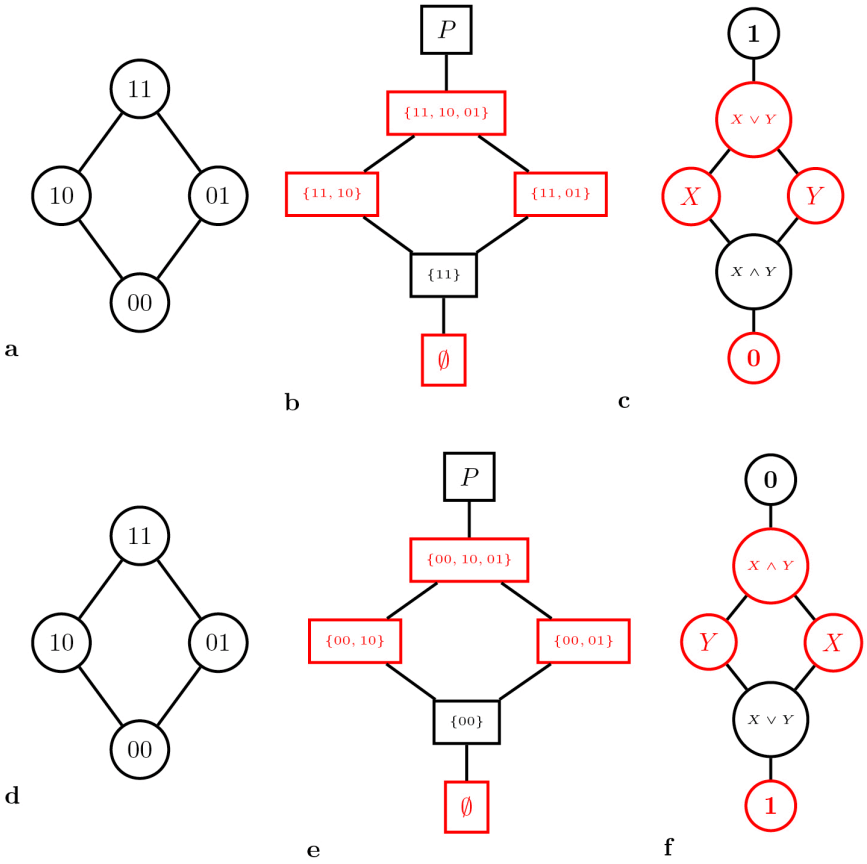

Fig 5. (a) Poset *P*; (b) Lattice of up-sets of *U*(*P*); (c) The set of monotone Boolean functions with two inputs *MBF*(2) is isomorphic to *U*(*P*) via the map $f \to T(f)$). (d) Poset *P*; (e) Lattice of down-sets of *J*(*P*); (f) The set of monotone Boolean functions with two inputs $MBF^a(2)$ with anti-order is isomorphic to *J*(*P*) via the map $f \to \ker f$.

https://doi.org/10.1371/journal.pcsy.0000103.g005

3.3 Structure of MBF models that support fixed points

In this subsection, we use the lattice theory language to describe the sets $L(x), U(x) \subset MBF(k)$.

Proof of Lemma 2.11.

Proof. By Theorem 3.16, each set $U(x)$ is a prime filter in MBF(k). Since the logical function in k arguments X_i given by

$$m := \bigwedge_{i=1}^{k} X_i \in MBF(k)$$

has unique predecessor $\mathbf{0} \in MBF(k)$, m is joint-irreducible element in $MBF(k)$. Consequently, $\uparrow m$ is a prime filter and it contains all functions in MBF(k), except the function $\mathbf{0}$. Therefore, this is the maximal filter with size $|MBF(k)| - 1$. Finally, since $\mathbf{0}$ is the only function that evaluates to 0 on input $b = 1$, it follows that $\uparrow m = U(1)$.

Analogously, by Theorem 3.16 each set $L(x)$ is a prime ideal in MBF(k). The logical function in k arguments X_i given by

$$M := \bigvee_{i=1}^{k} X_i \in MBF(k)$$

has unique successor **1** $\in MBF(k)$, M is meet-irreducible element in $MBF(k)$ and $\downarrow M$ is a prime ideal that contains all functions in MBF(k), except the function **1**. Therefore, this is the maximal ideal with size $|MBF(k)| - 1$. Finally, since **1** is the only function that evaluates to 1 on input $\mathfrak{o}$, it follows that $\downarrow M = L(\mathfrak{o})$.

Proof of Theorem 2.12

Proof. Any state $b \in \mathbb{B}^N$ is supported by the monotone Boolean model $f = (f_1, \ldots, f_N)$ where f_i is a constant function $f_i = b_i$. Therefore, the set of models supporting b is non-empty.

The rest of the Theorem follows by realizing that the equilibrium supported by most MB models is one where for each component i, the monotone Boolean function f_i will be from the largest set $U(b) \subset MBF(k)$, or $L(b) \subset MBF(k)$. These sets were characterized in Lemma 2.11.

Proof of Lemma 2.15

Proof. By Theorem 2.14 the models $f = (f_1, \ldots, f_N)$ that support bistability between $d = \mathfrak{o}$ and $e = \mathfrak{i}$ satisfy

$$f_i \in L(\mathfrak{o}_{k_i}) \cap U(\mathfrak{i}_{k_i}) \qquad \text{for all } i.$$

Since $L(\mathfrak{o}_{k_i}) = MBF(k_i) \setminus \{\mathbf{1}\}$ and $U(\mathfrak{i}_{k_i}) = MBF(k_i) \setminus \{\mathbf{0}\}$ it follows that

$$L(\mathfrak{o}_{k_i}) \cap U(\mathfrak{i}_{k_i}) = MBF(k_i) \setminus \{\mathbf{0}, \mathbf{1}\}.$$

The size of this set is

$$|L(\mathfrak{o}_{k_i}) \cap U(\mathfrak{i}_{k_i})| = |MBF(k_i)| - 2.$$

By the complementarity property in Theorem 3.6 that for any k and any $b \in \mathbb{B}^k$ the sets $U(b)$ and $L(b)$ satisfy

$$U(b) \cap L(b) = \emptyset \qquad \text{and} \qquad U(b) \cup L(b) = MBF(k).$$

Note, however, that if $U(b) = \uparrow g$ and $L(b) = \downarrow h$ then $g \neq h$ in general, see (Table 3).

We conclude with a result that is a direct consequence of Corollary 3.15. For illustration, see Table 3 for the table of all sets $U(b)$, $L(b)$ in MBF(3), which is depicted in Fig 6.

Lemma 3.17. *For any $b \in \mathbb{B}^k$ the sets $U(b), L(b) \subset MBF(k)$ satisfy*

$$|U(b)| = |L(\neg b)|$$

where $\neg$ is negation.

Table 3. Prime ideals (left) and prime filters (right) in MBF(3). Both sets are posets isomorphic to $\mathbb{B}^3$ by Birkhoff Theorem.

L(000)	$L(X \vee Y \vee Z)$	**19**	**U(000)**	$U(1)$	**1**
L(010)	$L(X \vee Z)$	14	U(010)	$U(Y)$	6
L(001)	$L(X \vee Y)$	14	U(001)	$U(Z)$	6
L(100)	$L(Y \vee Z)$	14	U(100)	$U(X)$	6
L(011)	$L(X)$	6	U(011)	$U(Y \wedge Z)$	14
L(101)	$L(Y)$	6	U(101)	$U(X \wedge Z)$	14
L(110)	$L(Z)$	6	U(110)	$U(X \wedge Y)$	14
L(111)	$L(\mathbf{0})$	1	U(111)	$U(X \wedge Y \wedge Z)$	19

https://doi.org/10.1371/journal.pcsy.0000103.t003

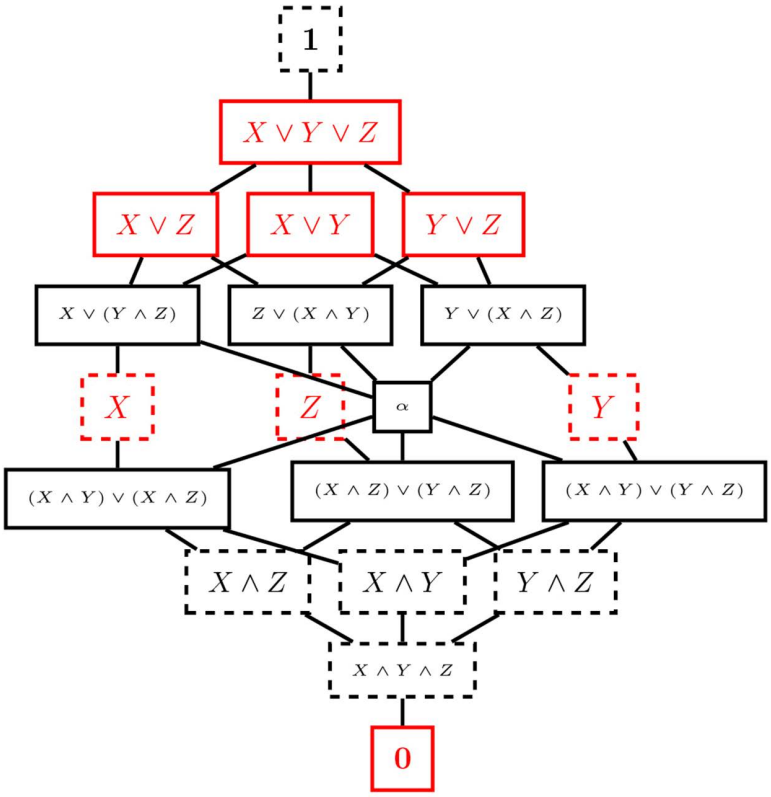

Fig 6. Lattice of monotone Boolean functions *MBF*(3). Nodes aligned horizontally have the same size of truth set, ranging from 0 at the bottom to $8 = 2^3$ on the top. Each node has DNF description of the function, where **0** and **1** are constant functions and $\alpha = (X \wedge Z) \vee (X \wedge Y) \vee (Y \wedge Z)$. Down-sets of meet-irreducible nodes (red) are the sets $L(*)$; while up-sets of join-irreducible elements (dashed) are the sets $U(*)$. Both collections are isomorphic to the poset $P = \mathbb{B}^3$..

https://doi.org/10.1371/journal.pcsy.0000103.g006

There are additional symmetries on the lattice $MBF(k)$, induced by permutations $p : \{1, \ldots, k\} \to \{1, \ldots, k\}$ on the set of coordinates for vectors $b \in \mathbb{B}^k$. Each such permutation p induces isomorphism $\pi : \mathbb{B}^k \to \mathbb{B}^k$. Since each function $f \in MBF(k)$ is uniquely determined by its truth set $T(f) \subset \mathbb{B}^k$, and the lattice operations are defined in terms of union and intersections of truth sets, the isomorphism π induces an automorphism

$$\Pi : MBF(k) \to MBF(k), \quad f \to g \tag{4}$$

where $T(g) = \pi(T(f))$.

Consider collection of prime ideals $\mathbb{L} := \{L(b) \mid b \in MBF(k)\}$ and collection of prime filters $\mathbb{U} := \{U(b) \mid b \in MBF(k)\}$. Each of these collections has 2^k elements, but the existence of this automorphism implies that these sets only have $k+1$ different sizes.

Theorem 3.18. *Consider collection of prime ideals* $\mathbb{L} := \{L(b) \mid b \in MBF(k)\}$ *and collection of prime filters* $\mathbb{U} := \{U(b) \mid b \in MBF(k)\}$. *Then there is a sequence of* $k+1$ *integers*

$$\beta_0^k < \beta_1^k < \beta_2^k < \ldots < \beta_k^k$$

with $\beta_0^k = 1, \beta_k^k = |MBF(k)| - 1$*, such that*

$$|U(b)| = \beta_j^k \quad \textit{where } j = \textit{ number of entries 1 in } b$$

$$|L(b)| = \beta_j^k \quad \textit{where } j = \textit{ number of entries 0 in } b$$

Proof. The fact that $\beta_0^k = 1, \beta_k^k = |MBF(k)| - 1$ follows from Lemma 2.11.

Consider any permutation $p : \{1, \ldots, k\} \to \{1, \ldots, k\}$ on the set of coordinates for vectors $b \in \mathbb{B}^k$ and the induced automorphism Π in (4).

It is easy to check that Π preserves the property of join- and meet-irreducibility and therefore induces an automorphism on the set $\mathbb{U}$. Since the map π preserves the number of 1s in the string, it follows that the size $|U(b)| = |U(\pi(b))|$. Therefore, the size of $|U(b)|$ only depends on the number of entries 1 in the string b.

Finally, since $MBF(k)$ is a collection of increasing monotone Boolean functions, then $b \prec c$ in $\mathbb{B}^k$ implies $U(b) \subset U(c)$ and thus $|U(b)| < |U(c)|$. This finishes the proof for the set $\mathbb{U}$. The result for the set $\mathbb{L}$ follows now from Lemma 3.17.

To illustrate the Theorem recall from Table 1 that for $MBF(2)$ the sizes of the sets $U(b)$, $L(b)$ are

$$\beta_0^2 = 1, \ \beta_1^2 = 3 \quad \text{and } \beta_2^2 = 5;$$

from Table 3 the sizes are

$$\beta_0^3 = 1, \ \beta_1^3 = 6, \ \beta_2^3 = 14 \quad \text{and } \beta_3^3 = 19.$$

Proof of Theorem 2.8

Proof. We order nodes $x_1, \ldots, x_N$. If there is no j such that f_j is decreasing in x_1, then all edges with source x_1 in the influence network are positive. We set $\alpha_1(x_1) := x_1$. Otherwise, if there is an f_j which is decreasing in x_1 we set

$$\alpha_1(x_1) = \neg x_1,$$

and for any f_k that depends on x_1 we have

$$f_k \text{ is increasing (decreasing) in } x_1 \leftrightarrow f_k \text{ is decreasing (increasing) in } \alpha_1(x_1). \tag{5}$$

However, since the update function for the node x_1 is $f_1(x)$ if we change variable x_1 to $\neg x_1$ we also need to change the sign of function f_1. In other words,

$$x_1 = f_1(x) \implies \alpha_1(x_1) = \alpha_1 f(\alpha_1(x_1), x_2, \ldots, x_N).$$

Setting $g_1 := \alpha_1 f_1$ it follows that

$$f_1 \text{ is increasing (decreasing) in } x_k \leftrightarrow g_1 \text{ is decreasing (increasing) in } x_k. \tag{6}$$

Consider now the influence network of a new model $\bar{f} = (g_1, f_2, \ldots, f_N)$ with state $(\alpha_1(x_1), x_2, \ldots, x_N)$. By (5) all influence edges of the original network f that start in x_1 have changed signs in the influence network of $\bar{f}$; and by (6) all influence edges that terminate in x_1 also changed signs.

Importantly, in any loop that passes through node x_1, there were two changes. Hence, the sign of the loop did not change, and we eliminated the negative edge from x_1 to x_j from the influence network. We conclude that the sign of every loop in the influence network of f is the same as in the influence network of $\bar{f}$.

We now consider the sources of node x_1 and ask if g_1 is decreasing in any of its inputs. If so, we list these inputs $I_1 := \{x_{j_1}, x_{j_k}, j_i < j_s\}$ when $i < s$ and apply transformation $\alpha_{j_i}(x_{j_i}$ in this order. This eliminates all negative edges until g_1 is increasing in all its inputs. Note that if g_1 is increasing in x_j no change is applied to x_j. We then move to sources of node x_{j_1} and eliminate all negative inputs to function g_{j_1}; then do the same x_{j_2} until all elements of I_1 are exhausted. If at any time all inputs are positive, we take the next node from the initial ordered list $x_1, \ldots, x_N$ that has not been considered in the previous steps.

Since there are no negative loops in the network RN when a previously considered node appears in the list of sources, it only can appear as a positive input, since the corresponding loop that has just formed will have all positive edges. As a result, no change will be required for such a node and every node in the list will be only handled once. Since there is a finite number of nodes in the network and we will only need to consider each of them for the change α only once, this process will terminate. Since every loop in the network RN is positive, the change of variables α will yield g with positive influence network.

4 Discussion

This paper presents a first step towards a mathematical understanding of the relationship between network structure and the dynamics it supports. The answer clearly depends on a class of models that is selected to represent the network dynamics; answering this question in the class of all differential equation models compatible with the network runs immediately into problems with basic concepts: What does it mean to have the same dynamics when both the class of models and the state space of every single model are uncountable?

We investigate this question within the class of monotone Boolean models where the set of models is finite (but large) and the state space is a finite set of Boolean vectors $\mathbb{B}^N$. In spite of this finiteness, Boolean models are very popular in systems biology as they combine the finiteness with sufficient expressiveness to capture qualitative dynamic behavior of regulatory networks.

We make two additional simplifications. First, we seek to describe the relationship between network structure and steady states, rather than more general dynamic behavior. Second, because we focus on steady states, we only consider balanced networks that do not contain negative loops. It is known [41] that negative loops are associated with the existence of attractors that consist of more than one state (for instance, complex attractors), and, in fact, the existence of such attractors requires negative loops in a network.

In networks with negative loops, some of the MBMs will not support any equilibria, only complex attractors, automatically decreasing the number of MBMs supporting a given equilibrium. This is consistent with results from the toggle triad, where the prevalence/stability of single high states is lower than the corresponding prevalence in two-team networks (balanced) networks [42]. This assumption, which excludes networks with negative loops, has been made for convenience, in order to describe the most common steady states and bistability. However, the description of models supporting steady states and multistability by up-sets and down-sets is applicable to any network structure. The work on understanding the connection between negative loops and complex attractors is the subject of our current work, and we believe that the approach outlined in this paper can be extended to general networks that contain negative loops.

Our results are consistent with work on the prevalence of steady states for the EMT network. Paper [43] found that positive loops are enhanced in the EMT network, which is consistent with the high prevalence of bistability in ODE simulations of EMT models. Two EMT models that are studied in this paper are balanced, and therefore, the E and M states are the most prevalent steady states across all MBM models for these networks. Further study of the robustness of this bistability was examined in [44]. This paper studied 13 different EMT networks and showed that while these wild-type networks

show the highest prevalence of E and M states in sampled ODE simulations, small perturbations of the network structure (i.e., change of edge sign) produced networks where the prevalence of E and M states decreased, and the prevalence of intermediate states increased. While our results do not directly address robustness under network perturbations, our results imply that among all networks with the same number of nodes and edges, the network that has all positive edges will have the highest prevalence of the constant $\mathtt{o}$ and $\mathtt{1}$ states. The removal of self-inhibition on SNAI1 simplifies our analysis of the EMT networks studied in this paper to a balanced network. Thus, E and M states are the most prevalent; any perturbation of this network that changes the signs of the edges will result in a network with decreased prevalence of E and M states and increased prevalence of the intermediate states. Unlike self-activation on ZEB, which has been experimentally demonstrated to maintain the M phenotype [45], the role of self-inhibition on SNAI1 has not been explored experimentally and is considered a noise buffer in ODE models [46]. While this exclusion may limit the biological accuracy of our model, it should have minimal impact on predictions of the Boolean models without noise considered here.

The realization that the sets of monotone Boolean functions that evaluate to either 0 or 1 as prime ideals or filters in the lattice of monotone Boolean functions with k inputs, allows us to prove general results that are valid for all k. This is significant since the size of $MBF(k)$ grows rapidly with k and it is only known for $k \leq 9$, but a construction of meet- and join-irreducible elements in $MBF(k)$ may be possible by inductive procedure from those elements in $MBF(k-1)$ in a way similar to the construction of $MBF(k)$ from $MBF(k-1)$ [17]. This in turn would enable explicit construction of monotone Boolean models with certain multistability properties, or, alternatively, prove that a particular network does not support multistability greater than some upper bound q.

We note that we allow monotone Boolean functions to have redundant inputs that do not affect the output of the function. Apart from the fact that inclusion of such functions allows monotone Boolean functions to form a lattice, such functions represent the parameter regimes where a gene can be constitutively activated or suppressed in certain tissue, or under some external condition.

Our approach can be compared to [47], which searches for all (locally) monotone Boolean models that satisfy a set of constraints imposed by partially observed data. These constraints include fixed point behavior, but also other attractors, as well as reachability and non-reachability between pairs of states. In both of our approaches, a model is considered valid if its influence graph is a subset of the given network graph. Chevalier et al. [47] encode the set of constraints into Answer Set Programming, a declarative programming used in difficult, often NP-hard, search problems, and then search for all models that satisfy them. Our approach considers only constraints given by the desired fixed points, but uses the explicit structure of the set of monotone Boolean models to compute the models with the desired behavior explicitly. In the future, we plan to extend our work from balanced to arbitrary networks, hoping to include more general attractors that arise in models of networks as a constraint.

Monotone Boolean function models are closely linked with ODE models with steep nonlinearities, which in the limit become *Glass models* with piecewise constant nonlinearities. Each such ODE model generates a finite state transition graph (STG) that encodes its dynamics, and there is only a finite collection of STGs that are compatible with the given network. This collection is organized in a DSGRN database, which takes the form of a graph [10,11]. Since MB network models are a subset of the DSGRN collection, the work presented here should describe multistability in ODE network models with steep nonlinearities. The precise nature of this connection is a subject of current investigation.

Reaction network theory takes a different approach to modeling network dynamics using mass action kinetics. The delineation of conditions that guarantee (or preclude) multistability has been a subject of many papers, see for instance [48–50].

The underlying philosophy of our approach, which aims to describe the full suite of network dynamics, is that important dynamics will occur with higher frequency within this set. The importance of particular network dynamics is weighted by the prevalence of MBMs that support it. That is, we view a steady state that is supported by 80% of all MBMs as more

important than a steady state that is only supported by 10% of all MBMs. It is certainly possible that biological control external to the network can keep the network in a (set of) MBMs which supports the dynamics with 10% prevalence, but in the absence of such information, we will assume that the more prevalent dynamics is more important.

Acknowledgments

Part of this work has been done while the last author visited Department of Bioengineering, Indian Institute of Science, Bengaluru, India. Its hospitality is gratefully acknowledged.

Author contributions

Conceptualization: Tomáš Gedeon.

Formal analysis: Sarah Adigwe, Harshavardhan BV, Tomáš Gedeon.

Investigation: Sarah Adigwe, Harshavardhan BV.

Visualization: Sarah Adigwe, Harshavardhan BV.

Writing – original draft: Sarah Adigwe, Harshavardhan BV, Tomáš Gedeon.

Writing – review & editing: Mohit Kumar Jolly, Tomáš Gedeon.

References

1. Hong T, Watanabe K, Ta CH, Villarreal-Ponce A, Nie Q, Dai X. An Ovol2-Zeb1 Mutual Inhibitory Circuit Governs Bidirectional and Multi-step Transition between Epithelial and Mesenchymal States. PLOS Computational Biology. 2015;11(11):e1004569. https://doi.org/10.1371/journal.pcbi.1004569
2. Huang B, Lu M, Jia D, Ben-Jacob E, Levine H, Onuchic JN. Interrogating the topological robustness of gene regulatory circuits by randomization. PLoS Comput Biol. 2017;13(3):e1005456. https://doi.org/10.1371/journal.pcbi.1005456 PMID: 28362798
3. Ríos O, Frias S, Rodríguez A, Kofman S, Merchant H, Torres L, et al. A Boolean network model of human gonadal sex determination. Theor Biol Med Model. 2015;12:26. https://doi.org/10.1186/s12976-015-0023-0 PMID: 26573569
4. Chang R, Shoemaker R, Wang W. Systematic search for recipes to generate induced pluripotent stem cells. PLoS Comput Biol. 2011;7(12):e1002300. https://doi.org/10.1371/journal.pcbi.1002300 PMID: 22215993
5. Udyavar AR, Wooten DJ, Hoeksema M, Bansal M, Califano A, Estrada L, et al. Novel Hybrid Phenotype Revealed in Small Cell Lung Cancer by a Transcription Factor Network Model That Can Explain Tumor Heterogeneity. Cancer Res. 2017;77(5):1063–74. https://doi.org/10.1158/0008-5472.CAN-16-1467 PMID: 27932399
6. Martínez-Antonio A, Janga SC, Thieffry D. Functional organisation of Escherichia coli transcriptional regulatory network. J Mol Biol. 2008;381(1):238–47. https://doi.org/10.1016/j.jmb.2008.05.054 PMID: 18599074
7. Zhang R, Shah MV, Yang J, Nyland SB, Liu X, Yun JK, et al. Network model of survival signaling in large granular lymphocyte leukemia. Proc Natl Acad Sci U S A. 2008;105(42):16308–13. https://doi.org/10.1073/pnas.0806447105 PMID: 18852469
8. Abou-Jaoudé W, Traynard P, Monteiro PT, Saez-Rodriguez J, Helikar T, Thieffry D. Logical Modeling and Dynamical Analysis of Cellular Networks. Frontiers in Genetics. 2016;7. https://doi.org/10.3389/fgene.2016.00094
9. Huang B, Jia D, Feng J, Levine H, Onuchic JN, Lu M. RACIPE: a computational tool for modeling gene regulatory circuits using randomization. BMC Syst Biol. 2018;12(1):74. https://doi.org/10.1186/s12918-018-0594-6 PMID: 29914482
10. Gedeon T. Multi-parameter exploration of dynamics of regulatory networks. Biosystems. 2020;190:104113. https://doi.org/10.1016/j.biosystems.2020.104113 PMID: 32057819
11. Cummins B, Gedeon T, Harker S, Mischaikow K, Mok K. Combinatorial representation of parameter space for switching networks. SIAM J Appl Dyn Syst. 2016;15(4):2176–212. https://doi.org/10.1137/15M1052743 PMID: 30774565
12. Font-Clos F, Zapperi S, La Porta CAM. Topography of epithelial-mesenchymal plasticity. Proc Natl Acad Sci U S A. 2018;115(23):5902–7. https://doi.org/10.1073/pnas.1722609115 PMID: 29784817
13. Chaouiya C, Naldi A, Thieffry D. Logical modelling of gene regulatory networks with GINsim. Methods Mol Biol. 2012;804:463–79. https://doi.org/10.1007/978-1-61779-361-5_23 PMID: 22144167
14. Stoll G, Caron B, Viara E, Dugourd A, Zinovyev A, Naldi A, et al. MaBoSS 2.0: an environment for stochastic Boolean modeling. Bioinformatics. 2017;33(14):2226–8. https://doi.org/10.1093/bioinformatics/btx123

15. Albert R, Thakar J. Boolean modeling: a logic-based dynamic approach for understanding signaling and regulatory networks and for making useful predictions. Wiley Interdiscip Rev Syst Biol Med. 2014;6(5):353–69. https://doi.org/10.1002/wsbm.1273 PMID: 25269159
16. Gedeon T. Network topology and interaction logic determine states it supports. NPJ Syst Biol Appl. 2024;10(1):98. https://doi.org/10.1038/s41540-024-00423-8 PMID: 39198512
17. Gedeon T. Lattice structures that parameterize regulatory network dynamics. Math Biosci. 2024;374:109225. https://doi.org/10.1016/j.mbs.2024.109225 PMID: 38866065
18. Korshunov AD. Monotone Boolean functions. Russ Math Surv. 2003;58(5):929–1001. https://doi.org/10.1070/rm2003v058n05abeh000667
19. Fidytek R, Mostowski AW, Somla R, Szepietowski A. Algorithms counting monotone Boolean functions. Information Processing Letters. 2001;79(5):203–9. https://doi.org/10.1016/s0020-0190(00)00230-1
20. Jäkel C. A computation of the ninth Dedekind number. Journal of Computational Algebra. 2023;6–7:100006. https://doi.org/10.1016/j.jaca.2023.100006
21. Mori T, Akutsu T. Attractor detection and enumeration algorithms for Boolean networks. Comput Struct Biotechnol J. 2022;20:2512–20. https://doi.org/10.1016/j.csbj.2022.05.027 PMID: 35685366
22. TAMURA T, AKUTSU T. Detecting a Singleton Attractor in a Boolean Network Utilizing SAT Algorithms. IEICE Trans Fundamentals. 2009;E92-A(2):493–501. https://doi.org/10.1587/transfun.e92.a.493
23. Dubrova E, Teslenko M, Ming L. Finding Attractors in Synchronous Multiple-Valued Networks Using SAT-Based Bounded Model Checking. In: 2010 40th IEEE International Symposium on Multiple-Valued Logic, 2010. 144–9. https://doi.org/10.1109/ismvl.2010.35
24. Beineke LW, Harary F. Consistency in marked digraphs. Journal of Mathematical Psychology. 1978 Dec;18(3):260-9. Available from: https://linkinghub.elsevier.com/retrieve/pii/0022249678900548
25. Harary F, Palmer EM. Graphical Enumeration. Elsevier; 2014. Google-Books-ID: ZrvSBQAAQBAJ.
26. Harary F. On the notion of balance of a signed graph. Michigan Math J. 1953;2(2). https://doi.org/10.1307/mmj/1028989917
27. Shi G, Altafini C, Baras JS. Dynamics over Signed Networks. SIAM Rev. 2019;61(2):229–57. https://doi.org/10.1137/17m1134172
28. Diaz-Diaz F, Candellone E, Gonzalez-Casado MA, Fraxanet E, Vendeville A, Ferri I, et al. Signed Networks: theory, methods, and applications. arXiv; 2025. ArXiv:2511.17247 [physics]. Available from: http://arxiv.org/abs/2511.17247
29. Harary F, Norman RZ, Cartwright D. Structural Models: An Introduction to the Theory of Directed Graphs. Wiley; 1965. Available from: https://books.google.com/books?id=DbY9AAAAIAAJ
30. Hari K, Harlapur P, Saxena A, Haldar K, Girish A, Malpani T, et al. Low dimensionality of phenotypic space as an emergent property of coordinated teams in biological regulatory networks. iScience. 2025;28(2):111730. https://doi.org/10.1016/j.isci.2024.111730 PMID: 39898023
31. Hari K, Ullanat V, Balasubramanian A, Gopalan A, Jolly MK. Landscape of epithelial-mesenchymal plasticity as an emergent property of coordinated teams in regulatory networks. Elife. 2022;11:e76535. https://doi.org/10.7554/eLife.76535 PMID: 36269057
32. Pastushenko I, Brisebarre A, Sifrim A, Fioramonti M, Revenco T, Boumahdi S, et al. Identification of the tumour transition states occurring during EMT. Nature. 2018;556(7702):463–8. https://doi.org/10.1038/s41586-018-0040-3 PMID: 29670281
33. Gardner TS, Cantor CR, Collins JJ. Construction of a genetic toggle switch in Escherichia coli. Nature. 2000;403(6767):339–42. https://doi.org/10.1038/35002131 PMID: 10659857
34. Hebbar A, Moger A, Hari K, Jolly MK. Robustness in phenotypic plasticity and heterogeneity patterns enabled by EMT networks. Biophys J. 2022;121(19):3600–15. https://doi.org/10.1016/j.bpj.2022.07.017 PMID: 35859419
35. Xin Y, Cummins B, Gedeon T. Multistability in the epithelial-mesenchymal transition network. BMC Bioinformatics. 2020;21(1):71. https://doi.org/10.1186/s12859-020-3413-1 PMID: 32093616
36. Adigwe S, BV H, Gedeon T, Jolly MK. Characterization of monotone Boolean models supporting fixed points and multistability in balanced networks. Zenodo; 2026. Available from: https://doi.org/10.5281/zenodo.18682834
37. Aracena J, Richard A, Salinas L. Number of Fixed Points and Disjoint Cycles in Monotone Boolean Networks. SIAM J Discrete Math. 2017;31(3):1702–25. https://doi.org/10.1137/16m1060868
38. Stanley RP. Enumerative Combinatorics. vol. 1 of Cambridge Studies in Advanced Mathematics. 2nd ed. Cambridge: Cambridge University Press; 2011. Available from: https://www.cambridge.org/core/books/enumerative-combinatorics/3155CDE1D973D49F873BDE2EAF8D7651. https://doi.org/10.1017/CBO9781139058520
39. Lattices RS. Lattices and Ordered Sets. New York, NY: Springer. 2008. https://doi.org/10.1007/978-0-387-78901-9
40. Birkhoff G. On the combination of subalgebras. Math Proc Camb Phil Soc. 1933;29(4):441–64. https://doi.org/10.1017/s0305004100011464
41. Snoussi EH. Necessary Conditions for Multistationarity and Stable Periodicity. J Biol Syst. 1998;06(01):3–9. https://doi.org/10.1142/s0218339098000042
42. Duddu AS, Sahoo S, Hati S, Jhunjhunwala S, Jolly MK. Multi-stability in cellular differentiation enabled by a network of three mutually repressing master regulators. J R Soc Interface. 2020;17(170):20200631. https://doi.org/10.1098/rsif.2020.0631 PMID: 32993428
43. Nordick B, Hong T. Identification, visualization, statistical analysis and mathematical modeling of high-feedback loops in gene regulatory networks. BMC Bioinformatics. 2021;22(1):481. https://doi.org/10.1186/s12859-021-04405-z PMID: 34607562

44. Rashid M, Hari K, Thampi J, Santhosh NK, Jolly MK. Network topology metrics explaining enrichment of hybrid epithelial/mesenchymal phenotypes in metastasis. PLoS Comput Biol. 2022;18(11):e1010687. https://doi.org/10.1371/journal.pcbi.1010687 PMID: 36346808

45. Preca BT, Bajdak K, Mock K, Sundararajan V, Pfannstiel J, Maurer J, et al. A self-enforcing CD44s/ZEB1 feedback loop maintains EMT and stemness properties in cancer cells. International Journal of Cancer. 2015 Dec;137(11):2566-77. Publisher: John Wiley & Sons, Ltd. Available from: https://onlinelibrary.wiley.com/doi/full/10.1002/ijc.29642

46. Lu M, Jolly MK, Levine H, Onuchic JN, Ben-Jacob E. MicroRNA-based regulation of epithelial-hybrid-mesenchymal fate determination. Proc Natl Acad Sci U S A. 2013;110(45):18144–9. https://doi.org/10.1073/pnas.1318192110 PMID: 24154725

47. Chevalier S, Froidevaux C, Paulevé L, Zinovyev A. Synthesis of Boolean Networks from Biological Dynamical Constraints using Answer-Set Programming. In: 2019 IEEE 31st International Conference on Tools with Artificial Intelligence (ICTAI), 2019. 34–41. http://doi.org/10.1109/ictai.2019.00014

48. Dickenstein A, Millán MP, Shiu A, Tang X. Multistationarity in Structured Reaction Networks. Bull Math Biol. 2019;81(5):1527–81. https://doi.org/10.1007/s11538-019-00572-6 PMID: 30788691

49. Sadeghimanesh A, England M. Polynomial superlevel set representation of the multistationarity region of chemical reaction networks. BMC Bioinformatics. 2022;23(1):391. https://doi.org/10.1186/s12859-022-04921-6 PMID: 36167486

50. Conradi C, Feliu E, Mincheva M, Wiuf C. Identifying parameter regions for multistationarity. PLoS Comput Biol. 2017;13(10):e1005751. https://doi.org/10.1371/journal.pcbi.1005751 PMID: 28972969